Electric double-layer capacitance between an ionic liquid and few-layer graphene

Eri Uesugi[1], Hidenori Goto[1,2]*, Ritsuko Eguchi[1], Akihiko Fujiwara[3] & Yoshihiro Kubozono[1,2]

[1]*Research Laboratory for Surface Science, Okayama University, Okayama 700-8530, Japan*

[2]*Research Centre of New Functional Materials for Energy Production, Storage and Transport, Okayama University, Okayama 700-8530, Japan*

[3]*Japan Synchrotron Radiation Research Institute, SPring-8, Hyogo 679-5198, Japan*

Supplementary information

1. Determining the number of layers in graphene

It is well known that the layer number n of graphene is easily distinguished by optical contrast[1–5] using the value of green shift (GS) defined by GS ≡ (G_s - G_f) / G_s. Here, G_f and G_s are the green intensities in red/green/blue microscope colour images of few-layer graphene (FLG) and the substrate, respectively[4]. The GS value increases stepwise with n and has enabled the reliable estimation[4] of n from 1 to 3. We extended this method to determine the n of thicker graphene by a combination of optical, Raman, and atomic force microscopies. We prepared standard samples including different n in single flakes (Fig. S1a). The layer number from n = 1 to 14 in these samples was distinguished with atomic force microscopy (AFM) as shown in Fig. S1a. To confirm the validity of this estimation, we compared the result from AFM with the other known methods for evaluating n: optical contrast[1–5] (Figs. S1b-S1d) and Raman spectroscopy[6–9] (Figs. S1e-S1g). The n obtained with AFM is used as the horizontal values in Figs. S1c, d, f, g.

The GS value of each layer was evaluated using the graph shown in Fig. S1b. Fig. S1c shows the n-dependence of the GS values for the standard samples. In Fig. S1c, we draw the calculated curve for GS values using the equation in Ref. 2. Here, the GS value calculated for a wavelength at from 556 nm is drawn[2], showing good agreement with measurement. The red shift (RS) is similarly defined by RS ≡ (R_s - R_f) / R_s, where R_f and R_s are the red intensities of FLG and the substrate, respectively. The value of RS is plotted in Fig. S1d, but the n-dependence of the RS value is weaker than that of the GS value. The relative blue shift (not shown) is obscure for n < 10. The gradual increase of the GS and RS values[1,4] supports our estimation of n.

To crosscheck the estimation of n, we carried out Raman spectroscopy using incident light of wavelength 488 nm (Fig. S1e). The ratio of the Raman 2D and G band peaks, $I(G)/I(2D)$, which significantly depends on n, is plotted in Fig. S1f. This shows a gradual increase in $I(G)/I(2D)$ with n in the same manner as Ref. 7, indicating that our estimation of n with AFM is appropriate. In addition, we measured the n-dependence of the integrated intensity of the Raman peak at 520 cm^{-1} due to the Si substrate (Fig. S1g). The decay of intensity with n, signifying the scattering of the laser light in the FLG, also supports our estimation of n.

Thus, we ascertained the equivalence of all these methods for estimating n. In practice, we estimated the n of an arbitrary flake not by using AFM, but by fitting measured GS values to the curve in Fig. S1c.

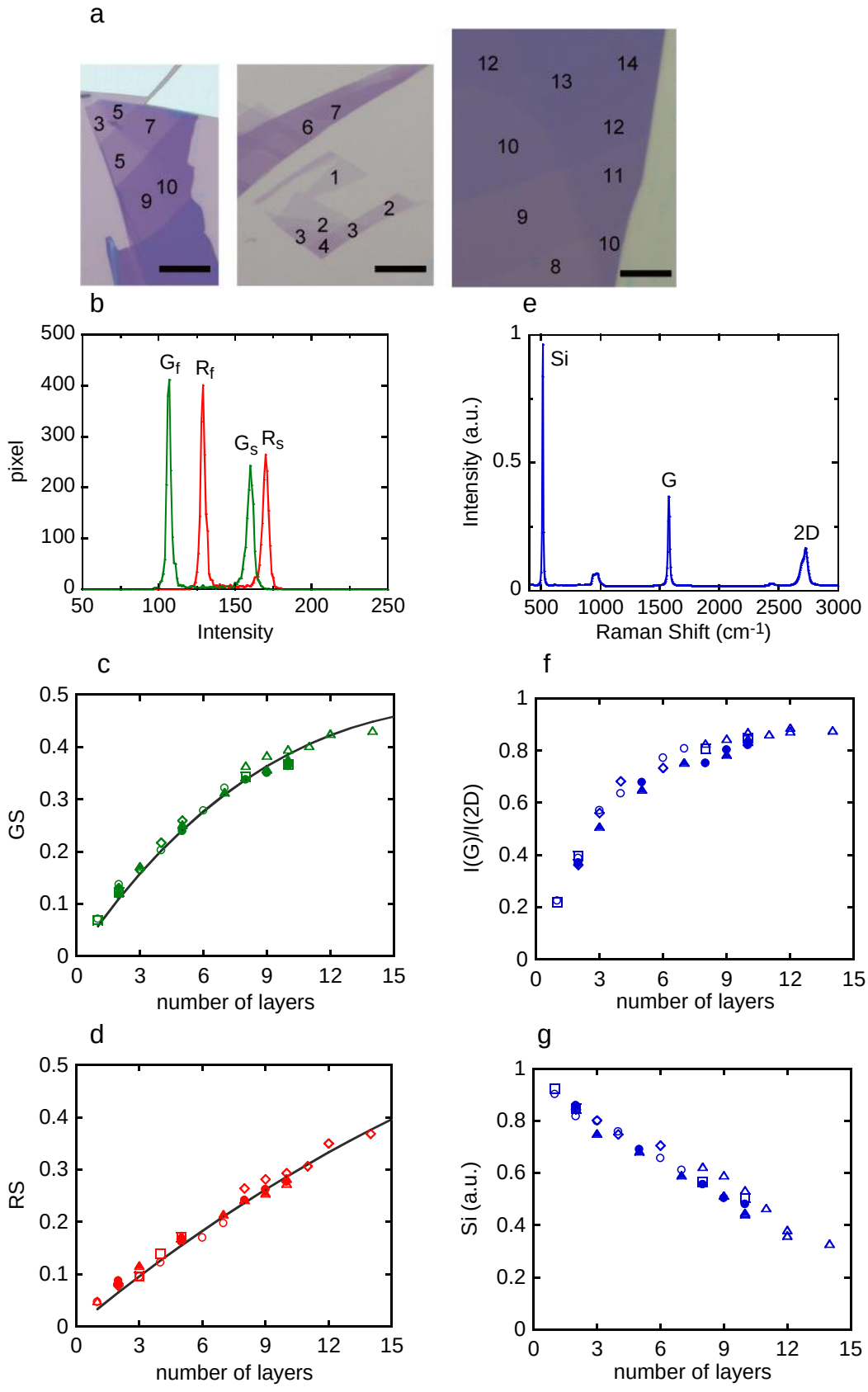
a
3 5 7 5 9 10
6 7 1 2 3 2 4 3
12 13 14 12 10 11 9 10 8
b
pixel
Intensity
G_f R_f G_s R_s
e
Intensity (a.u.)
Raman Shift (cm^{-1})
Si
G
2D
c
GS
number of layers
f
I(G)/I(2D)
number of layers
d
RS
number of layers
g
Si (a.u.)
number of layers

Figure S1 Determining the number of graphene layers

a Optical images of graphene flakes with different *n*, as determined with AFM and noted in the figures. All scale bars are 10 μm. b Optical contrast of 8-layer graphene relative to substrate. The colour of optical images is split into three components (red, green, and blue), and the number of pixels in the image is plotted as a function of each colour intensity. Green and red lines correspond to green and red components, respectively. The values of G_s, G_f, R_s and R_f refer to the intensity shown in the graph. We estimated GS and RS values using the equation in the text. c, d *n*-dependence of the GS and RS values. The solid lines show the GS and RS values calculated for wavelengths of 556 and 668 nm, respectively. From the plots in Figs. c and d, we find that the green intensity is the most useful for determining *n* because the optical contrast between FLG and the substrate is most prominent for that colour. e Raman spectrum of 8-layer graphene. The locations of G and 2D band peaks due to graphene and the peak due to the Si substrate are shown in the figure. f *n*-dependence of the relative intensity of the G and 2D band peaks. The ratio of integrated intensities is also useful for evaluation of *n*. g *n*-dependence of the integrated peak intensity around 520 cm^{-1} originating from the Si substrate. We find that the peak intensity due to the Si substrate decreases significantly with increasing *n* in the range of $n = 1$ to 14, which provides another indicator of *n*. As described in the text, the *n* obtained with AFM is used for the horizontal values in Figs. S1c, d, f, g.

2. Transport measurement with Hall bar devices

To confirm the validity of the result in two-terminal measurement, we studied the electric double-layer capacitance, C_{EDL}, using multi-terminal Hall bar devices. The optical microscope image of a Hall bar device is shown in Fig. S2a. The devices were prepared by the micromechanical cleavage of bulk graphite, followed by the fabrication of electrodes using the electron beam lithography and metal deposition. After that, the graphene was etched to a Hall bar shape using oxygen plasma. The current, I, and voltage, V_{xx} and V_{xy}, terminals are indicated in Fig S2a. The sheet conductivity and the Hall coefficient are obtained by $\sigma = LI / WV_{xx}$ and $R_H = V_{xy} / IH$, respectively. Here L and W are channel length and width, and H is magnetic field perpendicular to the device.

By substituting the above σ and R_H into the equations,

$$\mu = |\sigma R_H| \tag{S1}$$

and

$$en_e = CV_g = -1/R_H \text{ (or } en_h = -CV_g = 1/R_H), \tag{S2}$$

the mobility, μ, and the electron (hole) density, $n_{e(h)}$, were evaluated without any assumption. The equations (S1) and (S2) hold in the doped region where either electrons or holes present. First, C_{EDL} was estimated from the slope of $1/R_H$ - V_{tg} curve in the range where eq. (S2) holds. The values of C_{EDL} evaluated from the eq. (S2) are plotted in Fig. S2b. The trend of $C_{EDL}(n)$ is very similar to that estimated from two-terminal measurement shown in Fig 1a, proving the validity of the analysis in two-terminal measurement. Second, by measuring the σ and R_H for back- and top-gate voltage, V_{bg} and V_{tg}, separately, the mobilities for back- and top-gate, μ_{bg} and μ_{tg}, were

independently evaluated as a function of the hole density, n_h. The mobility ratio, $\mu_{bg}(n_h)$ / $\mu_{tg}(n_h)$ was calculated over the range from n_h^{min} to n_h^{min} + 10^{12} /cm^2. Here, n_h^{min} is the lowest n_h where eqs. (S1) and (S2) hold. The μ_{bg} / μ_{tg} is plotted as a function of n in Fig. S2c. The error bars reflects the standard deviations of σ and R_H measured in the range from n_h^{min} to n_h^{min} + 10^{12} /cm^2. The value of μ_{bg} / μ_{tg} is almost constant ~ 0.5 in this analysis, but is probed to be ~ 1 in two-terminal measurement. This difference may result from the contact resistance as describe in the main text.

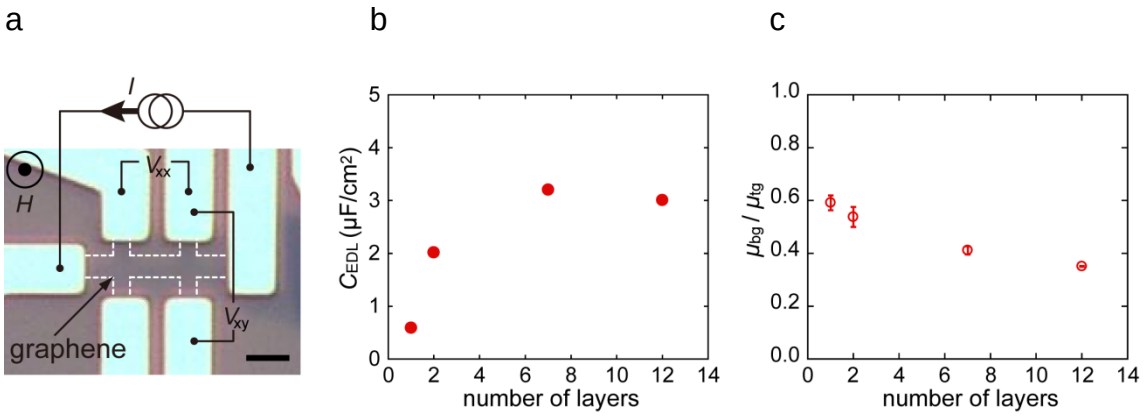

Figure S2 C_{EDL} obtained by 4-terminal transport measurement

a Optical microscope image of a device consisting of bilayer graphene. The device has a Hall bar structure indicated by dashed lines. The configuration of measurement terminals is indicated. Scale bar shows 2 μm. b C_{EDL} plotted as a function of n. c mobility ratio plotted as a function of n.

3. Charge distribution in FLG

The charges induced by the ionic liquid gate are distributed in FLG so as to minimize the total energy, $U_{EDL} = U_g + U_q$. The method used to determine the charge distribution was essentially the same as that in Ref. 10. For simplicity, we assumed a constant density of states at the charge neutrality point for $n \geq 2$. The density of states was calculated for ABA stacking FLG as described in Ref. 11. For SLG, we used the $C_q = e^2D(E)/2$, where $D(E)$ is the density of states at the charge density is 2×10^{12} cm^2. The calculated charge distribution in FLG is plotted in Fig. S3. Beyond 4 layers, the FLG does not show any meaningful change in charge distribution. This means that the electric field is screened within 4 graphene layers.

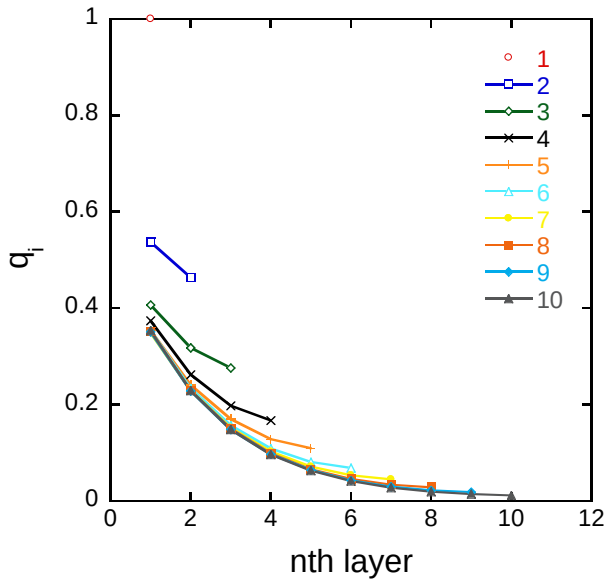

Figure S3 Calculation of charge distribution in FLG

The charge distributions in n-layer graphene for n = 1 to 10 are plotted as a function of layer position, numbered from the side of the ionic liquid. The total charge in each n-layer graphene is normalized to unity. For n > 4, no significant difference is observed.

4. EDL capacitance between FLG and an ionic liquid with large geometrical capacitance

To explore the possibility of high-density carrier accumulation, we calculated C_q, C_g and C_{EDL} for a virtual ionic liquid with a large C_g (C_g = 89 μF/cm^2) such as emimDCA[12]. The result is shown in Fig. S4. Even if the ionic liquid has a large C_g, C_{EDL} is limited by C_q for small n. With increasing n, C_g decreases significantly and C_{EDL} consequently remains a low value. This result indicates that high carrier density accumulation in FLG is difficult even using an ionic liquid gate.

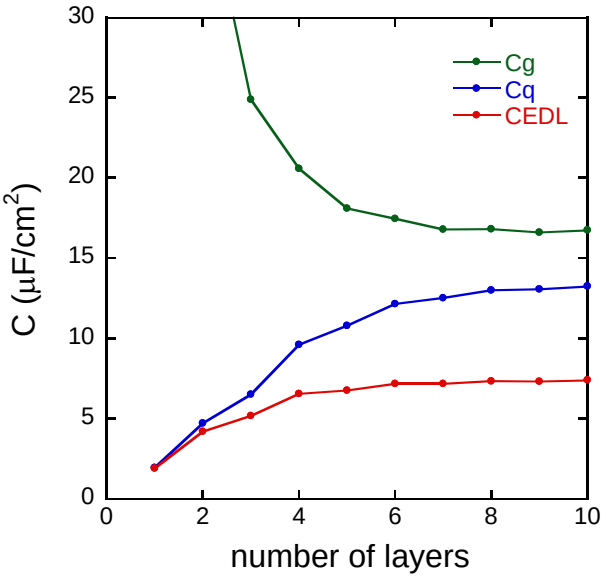

Figure S4 C_g, C_q, and C_{EDL} between n-layer graphene and an ionic liquid with extremely thin EDL

In this calculation, a virtual ionic liquid with C_g = 89 μF/cm^2 is used. C_g decreases significantly with n.

References

1. Blake, P. *et al.* Making graphene visible. *Appl. Phys. Lett.* **91**, 063124 (2007).

2. Ni, Z. H. *et al.* Graphene thickness determination using reflection and contrast spectroscopy. *Nano Lett.* **7**, 2758–2763 (2007).

3. Oostinga, J. B., Heersche, H. B., Liu, X., Morpurgo, A. F. & Vandersypen, L. M. K. Gate-induced insulating state in bilayer graphene devices. *Nature Mater.* **7**, 151–157 (2008).

4. Craciun, M. F. *et al.* Trilayer graphene is a semimetal with a gate-tunable band overlap. *Nature Nanotech.* **4**, 383–388 (2009).

5. Ye, J. *et al.* Accessing the transport properties of graphene and its multilayers at high carrier density. *Proc. Natl. Acad. Sci. USA* **108**, 13002–13006 (2011).

6. Ferrari, A. C. *et al.* Raman Spectrum of Graphene and Graphene Layers. *Phys. Rev. Lett.* **97**, 187401 (2006).

7. Graf, D. *et al.* Spatially resolved Raman spectroscopy of single- and few-layer graphene. *Nano Lett.* **7**, 238–242 (2007).

8. Gupta, A., Chen, G., Joshi, P., Tadigadapa, S. & Eklund, P. C. Raman scattering from high-frequency phonons in supported *n*-graphene layer films. *Nano Lett.* **6**, 2667–2673 (2006).

9. Malard, L. M., Pimenta, M. A., Dresselhaus, G. & Dresselhaus, M. S. Raman spectroscopy in graphene. *Phys. Rep.* **473**, 51–87 (2009).

10. Kuroda, M. A., Tersoff, J. & Martyna, G. J. Nonlinear screening in multilayer graphene systems. *Phys. Rev. Lett.* **106**, 116804 (2011).

11. Koshino, M. Interlayer screening effect in graphene multilayers with ABA and ABC stacking. *Phys. Rev. B* **81**, 125304 (2010).

12. Ono, S., Miwa, K., Seki, S. & Takeya, J. A comparative study of organic single-crystal transistors gated with various ionic-liquid electrolytes. *Appl. Phys. Lett.* **94**, 063301 (2009).